Seismic hazard analysis of complex faults using Spectral element and empirical Green's function methods

David Castro-Cruz, F Lopez-Caballero, Filippo Gatti

17th World Conference on Earthquake Engineering, 17WCEE
Sendai, Japan - September 13th to 18th 2020

Seismic hazard analysis of complex faults using Spectral element and empirical Green's function methods

D. Castro-Cruz[1], F. Lopez-Caballero[2], F. Gatti[3]

[1] *Researcher, LMSSMat UMR CNRS 8579 – CentraleSupélec – Université Paris Saclay, david.castro-cruz@centralesupelec.fr*
[2] *Assistant Professor, LMSSMat UMR CNRS 8579 – CentraleSupélec – Université Paris Saclay, fernando.lopez-caballero@centralesupelec.fr*
[3] *Associate Professor, LMSSMat UMR CNRS 8579 – CentraleSupélec – Université Paris Saclay, filippo.gatti@centralesupelec.fr*
…

Abstract

Seismic ground motion is strongly affected by many phenomena depending on complex characteristics, some of them related to the source. Those phenomena must be taken into account in risk mitigation, for example through the evaluation of several simulations for a future fault scenario. However, each analysis has high computational cost in the case of physical-based numerical models, even with efficient numerical methods such as Spectral Elements Method (SEM). It makes difficult to evaluate more than dozens of alternatives with high refined mesh with SEM. In this work an alternative method is proposed, it takes advantage of the results from few SEM simulations, and by combining it with the Empirical Green Function method (EGF), we are able to evaluate thousands of alternatives that could affect a region. This combination of methods allows us also to recreate simulations at low and high frequencies as well with a reduce cost.

This work focuses on the variability of some fault parameters, including stress drop and rupture geometry. Joining SEM and EGF methods, we analyzed the seismic hazard to the nuclear site of Cadarache, France. We use SEM method to simulate the ground motions for several point sources around the fault of Middle Durance (Southeastern zone). These results are combined and scaled by the EGF method, allowing to build with few SEM simulations the ground motions for thousands of simulation with different fault parameters. Those simulations are usually valid for low frequencies where the mesh is refined enough. At high frequencies, we employ the well-known method of EGF using previous records in the zone coming from the same fault. EGF method recreates several alternatives taking into account the variability of the source with empirical methods. The combination of both methods results in broad band accelerograms and it allows to consider several alternatives of faults in the seismic hazard analysis.

Here, we are presenting our procedure and the precautions to be taken into account for combining SEM and EGF methods. The obtained results are showing the usefulness of considering the fault variability to better predict the seismic hazard in region.

Keywords: Earthquake simulation; ; Seismic hazard; Empirical Green function; Spectral Element Method; SEM3D

1. Introduction

The purpose of this work is to determinate the ground motion generated by possible earthquakes. We use the Empirical Green function method [1] for evaluating different scenarios using records of weak earthquakes. We use also spectral element model to generate synthetic Green function (SGF) [2,3]. In this case we use the Spectral Element Method (SEM) [4] for generating the SGF, including 3D geometry and taking in account a complex 3D geology. We propose to mix both methods, since the frequency range of application in each method is often different. This allows us to reproduce the broad band ground motions with a wide frequency range.

The region of Cadarache is localized in the south-east of France (Fig. 1). This zone present complex geological formation that includes several faults that represent a seismic risk. This study evaluates mainly a close active fault that was discovered as reactivated fault in the last years [5]. We use numerical model using SEM, to build earthquake scenario in the region. For building this model, we integrate geological information, including a distinguish model for the basin around the structures. We include also the topography of the region since the region presents a complex topography with a mountain chain close to a valley. Integrating those items in a 3D numerical model, we quantify the seismic risk, by a stochastic analysis, at the region in the Cadarache for Mw 6.0 earthquake at 17.5 km away from the basin (see location in Fig. 1).

2. Empirical Green Function method (EGF)

Empirical Green's function (EGF) methods have been widely used because they enable to reproduce temporal signals taking into account path and site effects realistically [6]. Generally, this approach takes advantage of real signals of small earthquakes to produce realistic ground motions coming from some earthquake from a similar tectonic context.

A methodology that combines the procedure of Kohrs-Sansorny et al., (2005) [1] with the analysis of the source duration of global earthquakes presented in Courboulex et al., (2016) [7] with the SCARDEC database [8]. This methodology proposes a density function for the corner frequency depending of the seismic moment and the kind of source of the model. A detailed explanation can be found in Castro-Cruz, (2018) [9]. In general, a seismic ground motion at any point can be obtained by:

$$S(f) = STF(f) \cdot Pa(f) \cdot TF(f) \tag{1}$$

Where S is the spectrum of the modulated ground motion, STF is the source function, Pa the path contribution, and TF is the transfer function that quantifies the site effects. If the system is linear, then for a strong motion coming from the same location than a weak ground motion, the path effects (P) and site effects (TF) are the same. Then from Eq. (1) we obtain that the deconvolution between strong and the weak events (R) as:

$$R = {S^{\{EGF\}}}_{strong} \Big/ S_{weak} = STF_{strong} \Big/ STF_{weak} \tag{2}$$

Meaning that the deconvolution (R) between the ground motions of the strong (${S^{\{EGF\}}}_{strong}$) and weak event (S_{weak}), it is equal to the deconvolution of the weak source time function (STF_{weak}) and the strong one (STF_{strong}). Note that we use the convention ${S^{\{EGF\}}}_{strong}$ to indicate that we are using EGF method to estimate the ground motion from the strong earthquake. Using this equivalence, many methods are proposed to compute ${S^{\{EGF\}}}_{strong}$ from an estimation of R. Kohrs-Sansorny et al., (2005) [1] proposes the Eq. (3) to estimate R.

$$r^{\{i\}}(t) = \kappa \sum_{d=0}^{n_c} \left[\sum_{c=0}^{n_d} \delta(t - t_c - t_d) \right] \tag{3}$$

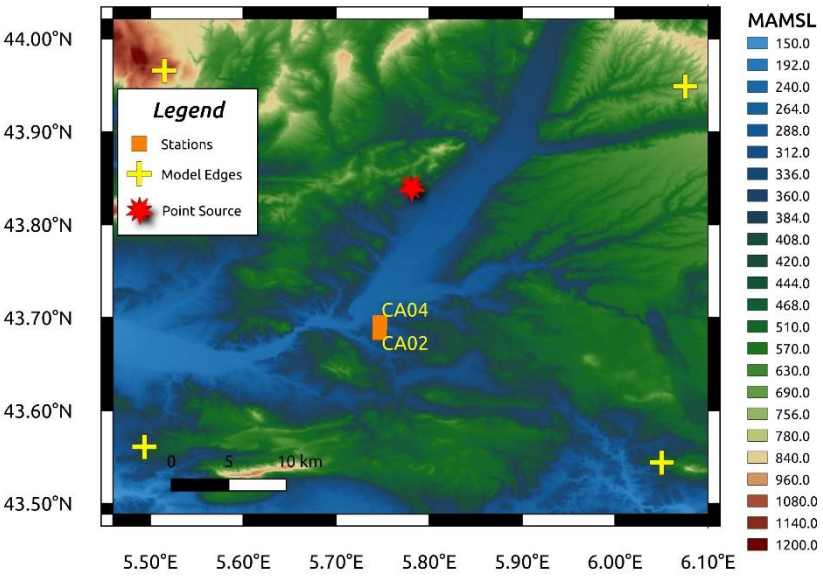

Fig. 1 - Zone of Cadarache with the point source earthquake and the stations analyzed in this study. The color map shows the meters about the mean sea level.

The Eq (3) comes from assuming that the earthquake sources follow the ω^2 model. $r^{\{i\}}$ is a temporal realization between the possible alternatives that keep the relationship in the Eq (1). The mean spectrum between all the realization $r^{\{i\}}$, that are temporal function of R, satisfies the Eq. (2). The components t_c and t_d are temporal lags randomly generated. Those lags allow to obtain realization $r^{\{i\}}$ that are different, realistic, and satisfying the Eq. (2) in average. Finally, in Eq. (3) δ is the Dirac's function and η_c and η_d are the number of impulses for making $r^{\{i\}}$. To choose η_c, η_d, and the density function for t_c and t_d, we follow the methodology presented in Castro-Cruz, 2018 [9]. In this methodology, we use a database of source time functions for generating a distribution of probability for those parameters.

We applied this EGF method to the case of Cadarache. We use as weak event M_L 2.9 earthquake occurred the 8th July 2010. The seismic moment was taken as 1.8 10^3 Nm. The strike, dip and rake of this earthquake are 186°, 19°, and -90°. The location of the earthquake is 43.940°N and 5.781°E with a depth of 3490 m (see the earthquake position in Fig. 1). The parameters of this event were taken from Dujardin et al (2019) [10]. The Corner Frequency (fc) was selected directly from the records as 2.7 Hz.

Using the parameters mentioned before, we obtain 5000 realizations for $r^{\{i\}}$. Fig. 2 shows two examples of realizations $r^{\{i\}}$ with different corner frequency (Fc). Those functions have different shapes and duration (due in part to the corner frequency) for each realization. Those changes between realizations recreate the variability in the source of an earthquake.

Using Eq. (2) we find the spectra for new ground motions convolving the accelerogram of weak motion with the scale function r (Eq. (3)). With this, we compute the ground motion at surface due to earthquakes with each realization $r^{\{i\}}$. Fig. 3 shows the accelerograms at the station CA04 (Fig. 1) with the sources of Fig. 2. The difference in the duration of the rupture, they cause that the event with *Fc* of *0.175Hz* has a higher amplitude than the other case with lower *Fc*.

The predicted ground motion by EGF method (Fig. 3) is limited to the frequency range where the weak ground motion is well recorded. Usually, the weak ground motion records have a limitation at low frequencies because the noise. In the case of Cadarache, the EGF prediction must be considered valid between *1 Hz* to *15 Hz*.

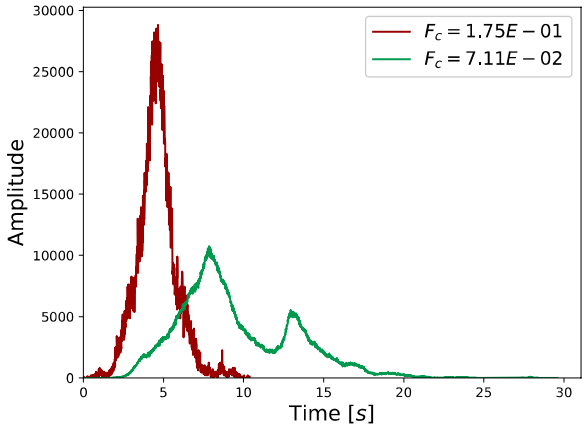

Fig. 2 – Two realizations ($r^{\{i\}}$) that generate different source time functions using different corner frequencies (Fc).

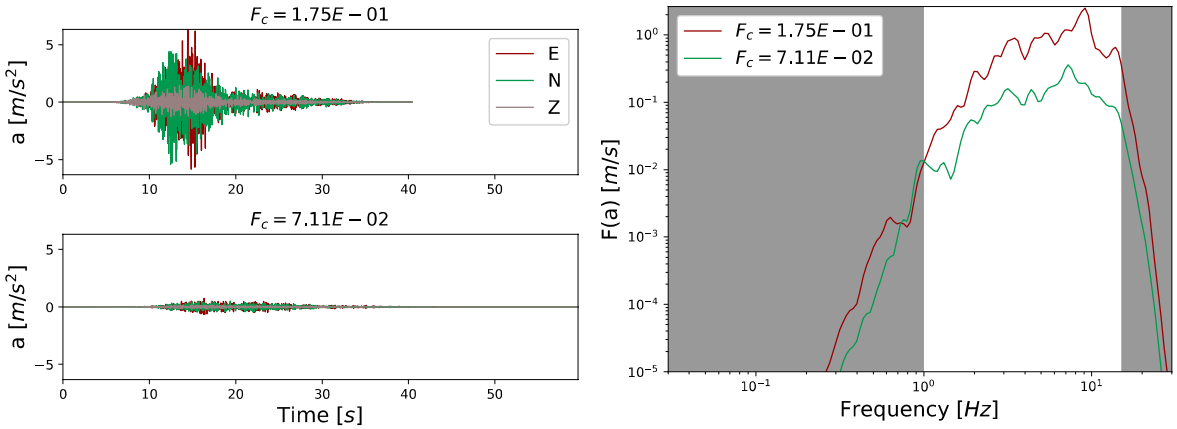

Fig. 3 - Ground motion at the station CA04 for two simulation with different STF (Fig. 2). Temporal accelerograms (left) and horizontal spectrum (right). Gray area shows the application zone of the filter.

3. Synthetic Green Function (SGF)

We use SEM method to build a synthetic Green's function (SGF). Those SGF allows us to model different earthquake scenarios with limited computational cost. This method of SGF starts by the selection of the location of "n" number of SGF. Those points must cover the extension of the target sources. In this paper, we present the method with a point source, meaning that we use a unique SGF in the simulation.

In the theoretical method of Green's functions, the pulse is defined by the Dirac's delta. However, it is not possible to define the Dirac's delta in a discrete formulation that can be used in a numerical model. We then must select a pulse that covers the frequency range that we are interested. In the case of this study, we select a frequency window between 0.1 Hz to 30 Hz and the we choose a Gabor wavelet (Eq. (4)).

$$p = Ae^{-(\sigma/\gamma)^2} \cdot \cos(\sigma) \tag{4}$$

Where A is the amplitude of the pulse, defined as 10^{11} Nm, σ is a time-frequency parameter ($\sigma = 2 \cdot \pi \cdot fc(t - t_o)$), with f_c equal 15 Hz, t_o equal 0.5 s and γ is 0.1. The pulse function covers uniformly the window of frequency that is searched in the simulation (see Fig. 4).

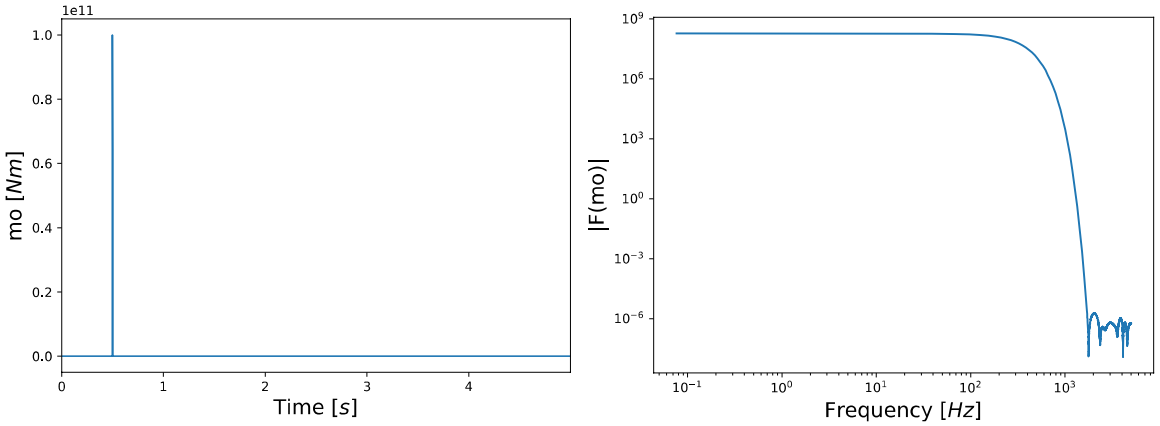

Fig. 4 - Time pulse (left) and spectrum of the pulse (rigth) that utilize for generating the SGF.

A seismic moment is introduced in the position 5.7810°E, 43.8398°N and -3039 m with respect to the sea level (red star in Fig. 1). For modeling this SGF, we use a mesh of 19' 448 496 elements with 3 point of integration (Gll), arriving to 526 million of freedom degrees. As boundary conditions, we use Perfec Matched Layers (pml) method [11] with a length of 3000 m and order 2.

3.1 Geology and mesh of the SEM model

At each point the parameters of shear velocity (Vs), compression velocity (Vp), and density (ρ) are defined in function of the depth (The geological model was provided by the commission of atomic energy, CEA by the acronym in French). There are two models, one for the general zone, and another for the zone close to the buildings where we consider a basin.

Outside of the basin, the mechanical properties are defined with the functions in Fig. 5. This functions were defined by CEA with seismic campaigns on the field.

In Fig. 5, z' represents the depth that is computed at each point using the DEM of the zone (Fig. 1). The first layer of the equations, that corresponds to the first 60 m of depth, it is just applicable to the zone around the basin, inside 1km of distance to the basin.
The final mechanical properties in the zone are shown in the Fig. 6 for the case of shear velocity. In this figure we observe three parts, one with high shear velocity at surface (3200 m/s) that uses the bedrock model (Fig. 5) without the first layer of 60 m. The second part with Vs of 1000 m/s at surface uses also the bedrock model but with all the layers. Finally, the last part is the basin (see Fig. 5) and corresponds to the zone of Cadarache basin.

Using SEM3D, we obtain the accelerograms at the stations CA02 and CA04 (Fig. 1) with the pulse source. Those accelerograms (see Fig. 7) were filtered until 4 Hz.

3.2 SGF convolution

This method [3] has several similitudes with the EGF method briefly explained in the previous subsection. In this work, using the spectral element method and the mentioned parameters before, we build a model for simulating a pulse function (Fig. 4). We obtain the accelerograms at the zone of interest. Those accelerograms are used as Green's functions. Hartzell, (1978) [6] proposed to use empirical Green's function replacing the source by the deconvolution between the source time function of the strong event (STF_{strong}), and the source that produces the accelerogram we use as Green's function. Applying this to the case of *SGF* method, we obtain:

$$S^{\{SGF\}}{}_{strong}(f) = SGF \cdot \frac{STF_{strong}}{P} \qquad (5)$$

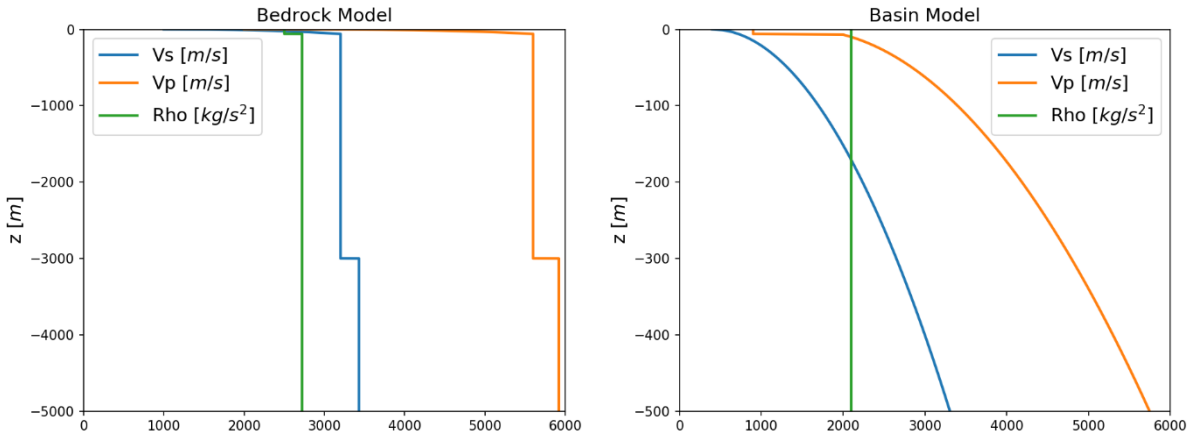

Fig. 5 - Definition of the soil mechanic parameters for the basin zone and the outcrop zone.

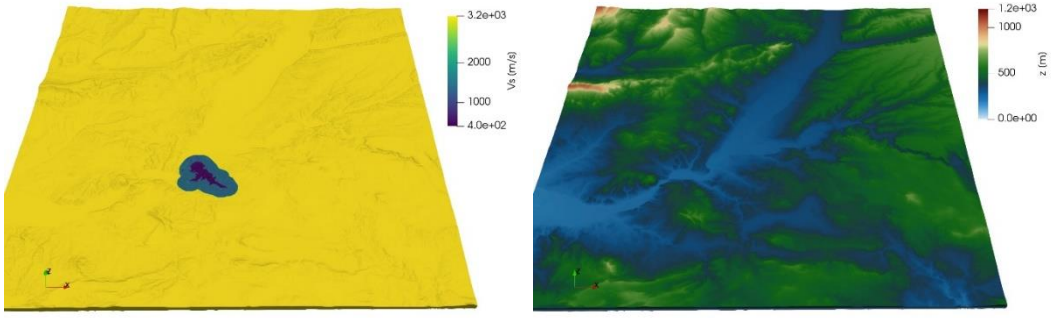

Fig. 6 - Shear velocity on the model (left) and topography (right). The basin zone has a Vs=400 m/s.

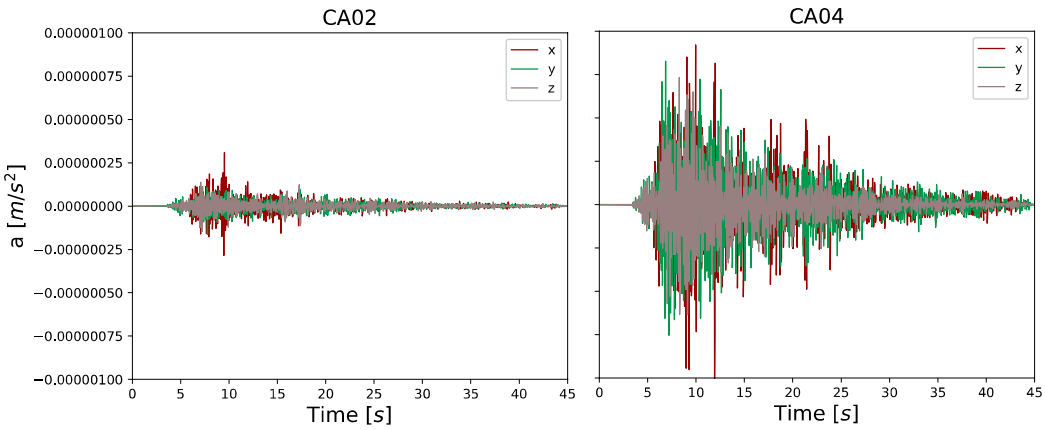

Fig. 7 - Ground motions at two stations using a SEM model. x: East-west direction, y: south north direction, and z: up-down direction.

Where. *SGF* is the synthetic Green's function, in our case the spectrum of the accelerogram that we compute using SEM. STF_{strong} is the Source time function of the event we simulate, and P is the spectrum of the pulse that generated the *SGF*. $S^{\{SGF\}}{}_{strong}(f)$ is the spectrum of the simulated ground motion with the strong earthquake, and we indicate in his name the SGF method. Using the *SGF* method, like the Green's function method, it is important to note that we are assuming a linear behavior of materials in the simulation.

We validate the method predicting the ground motions at the stations of interest CA02 and CA04 (see Fig. 1), and comparing the results with the ground motions that are computed directly form a simulation with SEM. The source is a Mw 6.0 earthquake from the same position that the Fig. 1 shows. We use the method of Kristeková et al. (2006, 2009) [12,13] to quantify the goodness of fitting between signals. The criteria stablish 10 as perfect fitting, but 8 indicates a very good fitting. In the case of the CA02 station at east-west and south-north directions, both models have a good fitting, although after 20 s there are small differences (Fig. 8).

Also, in the other components we obtain values with good fitting (Fig. 9). This results indicate that effectively, SGF method is equivalent to SEM simulation, taking in account effects as topography, and complex geology. However, SGF method has a lower marginal computational cost than SEM. SEM needed 10h05 for computing in a super calculator (fusion or occigen) with 720 MPI cores. SGF method took less than one second in a personal computer, although this time does not take in account the simulation of the SGF, that was done by a SEM model.

STF_{strong} in equation Eq. (5) can be any source time function we want to generate the new ground motion. In this study the objective is to complement the *EGF* method, then we must introduce the same source that the *EGF* simulates. To obtain the source time function that the *EGF* method (see section 2) we introduce in the Eq. (5) the Eq. (2):

$$S^{\{SGF,\ i\}}{}_{strong}(f) = R^{\{i\}} \cdot \frac{STF_{weak}}{P} \tag{6}$$

Where $R^{\{i\}}$ is the spectrum of the realization $r^{\{i\}}$ (Eq. (3)). STF_{weak} is the source time function of the earthquake we use as empirical green function. Finally, P is the spectrum of the pulse function for generating the SGF (Eq. (4)). Here we assume that STF_{weak} follows the ω^2-model [14,15].

Applying the Eq. (6) in Cadarache case we applied the method on the stations CA02 and CA04 (see Fig. 1). We take as SGF the ground motion during the simulation with the pulse (see Fig. 7). The Fig. 10 shows the case in the station CA04 using the same source function of the Fig. 2. Like the *EGF* case, the ground motion for a source with 0.175 *Hz* has higher amplitude than the ground motion from the source with Fc equal 0.0071 *Hz*.

4. Broad band simulations using EGF and SGF methods.

The EGF method is limited at low frequencies because small earthquakes do not generate enough energy at low frequencies to be correctly recorded at surface by the stations. In the case of SGF method, the frequency band depends of the accelerogram that the method uses as *SGF*. Using SEM, the high frequencies are limited by the accuracy of the numerical model, related with the size of the elements in the mesh. The proposed method in this section pretends to better take advantage of EGF and SGF methods to generate a unique simulation from both methods with a wide frequency band.

For each realization $r^{(i)}$ we obtain the ground motion by integrating SGF and EGF results. We propose to define a new ground motion as:

$$S^{\{i\}}{}_{strong}(f) = w(f) \cdot S^{\{SGF,\ i\}}{}_{strong} + (1 - w(f)) \cdot S^{\{EGF,\ i\}}{}_{strong} \tag{7}$$

Where $S^{\{SGF,\ i\}}{}_{strong}$ and $S^{\{EGF,\ i\}}{}_{strong}$ are obtained with SGF and EGF methods respectively (see Eq. (6) and (2)). The function *w* gives the weigh for each model for each frequency to compute the strong ground motion (S_{strong}). The function *w* gives higher weigh to the *SGF* method at low frequencies and the inverse at high frequencies (see Fig. 11). We define this function as:

$$w(f) = \frac{1}{1 + \left({}^{f}/_{m}\right)^{d}} \tag{8}$$

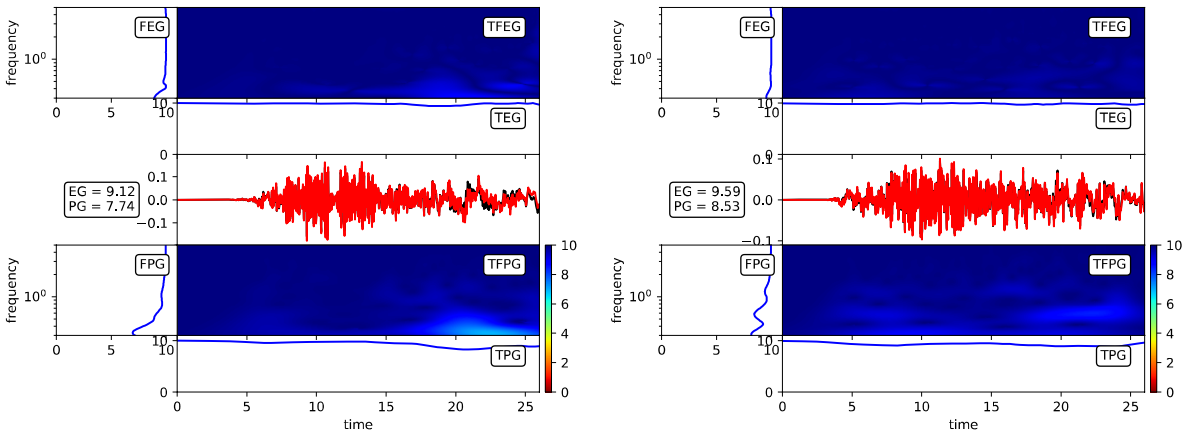

Fig. 8 - Evaluation of the goodness of fitting between the ground motions in east-west direction (left), and south-north direction (right) for a Mw 6.0 earthquake. Using SEM method (red line) and following SGF the method (black line), both ground motions are in CA02 station.

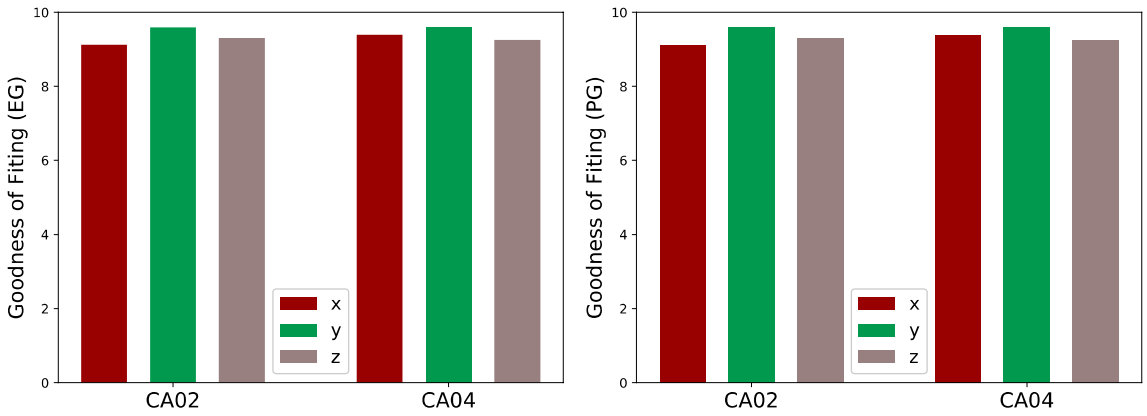

Fig. 9 - EG and PG values to evaluate the goodness of fitting between the two method, SEM and SGF.

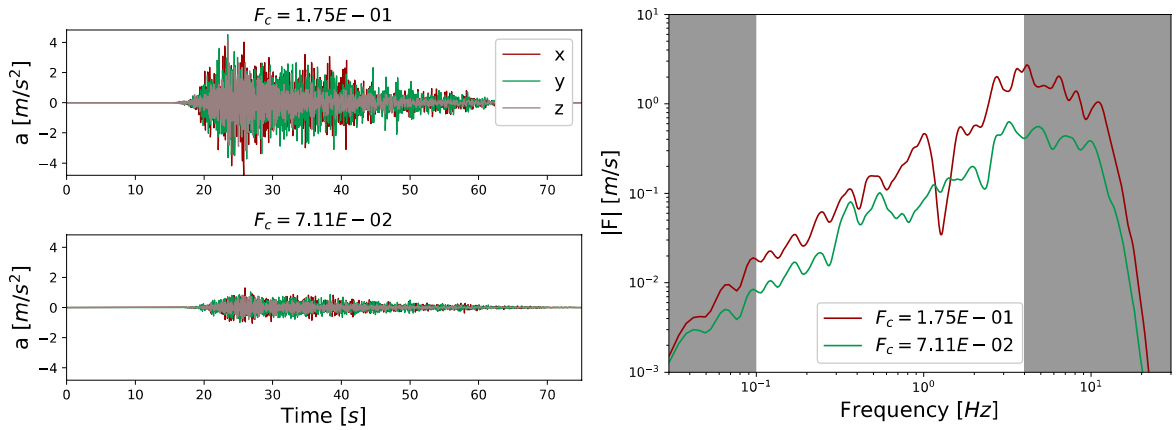

Fig. 10 - Example of two ground motions obtained by SGF method for different sources with Mw 6.0. This case shows the station CA04.

Where m and d are values fixed to fit the frequency range from each method. In the case of Cadarache, we define that *EGF* method has a high weigh before 1 Hz, and SGF method after 5 Hz (Fig. 11). In this case, we fix the values m and d, with $m = \sqrt{5 * 1}$ and $\log_{10} d = \log_{10}(\frac{5}{1}) / \log_{10}(7)$.

Applying the method and using the Eq. (7), we obtain the solution at the stations CA02 and CA04 for 5000 sources. The Fig. 11 shows as example the build accelerograms using the ground motions from EGF method (see Fig. 3), and SGF method (Fig. 10). Like the previous methods, we see a clear influence between using a source with a *Fc* of $1.75 \cdot 10^{-1}$ *Hz* and $7.11 \cdot 10^{-2}$ *Hz*.

Analyzing 5000 realization of sources, each one with different configuration of stress drop and different patrons in releasing the energy in the source time function, we build a stochastic analysis. The Fig. 13 shows the exceedance probability (E.P) for the PGA and the response spectra with a period of 0.65 s, using the same earthquake than previously (Mw 6.0, see Fig. 1). The average value, where E.P is equal to 0.5 (see Fig. 13), the analysis shows that in average the CA04 station has a higher intensity than CA02. This is congruent with the location of the stations, since CA04 is in the basin and CA02 in the outcrop.

The Fig. 14 shows the E.P for all the periods in the response spectra. E.P indicates that is more probable to have a higher intensity in all periods of the response spectra for the station CA04 than the station CA02. Fig. 14 shows that at the period of 0.4 s the station CA04 has the main peak of the response spectra, where the amplitude of the average reaches 10 m/s^2. In both stations in high periods (T>2.0s) there is not a representative peak, and the exceedance probability is almost zero for intensities upper than 0.2 m/s^2.

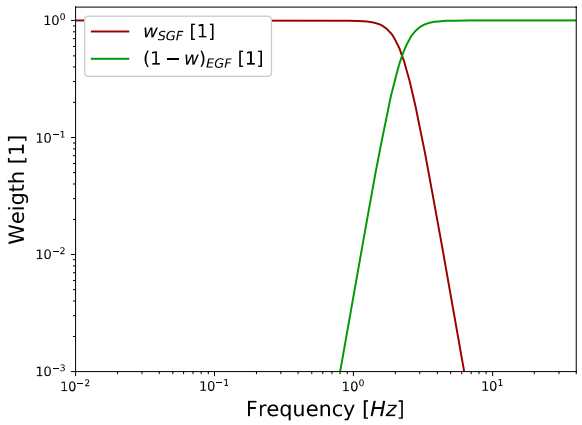

Fig. 11 - Function that gives the weight of the contribution from each model in the wide frequencies.

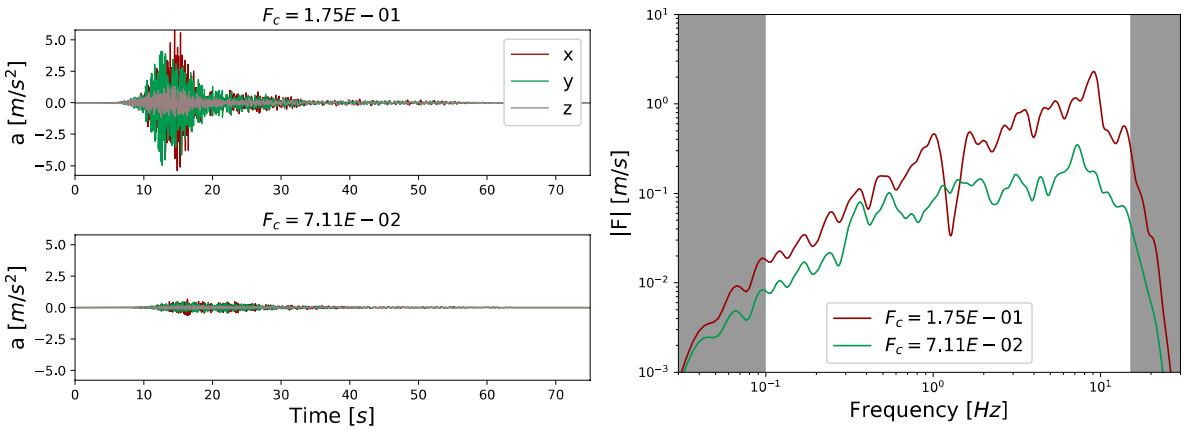

Fig. 12 - Ground motion simulation mixing EGF and SGF method for two different sources. Both simulations are at the station CA04.

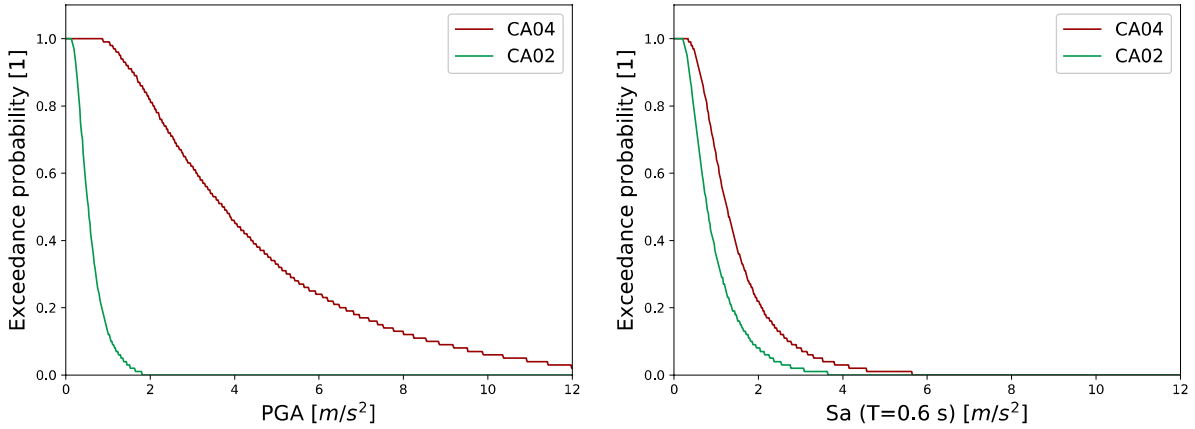

Fig. 13 - Probability of exceedance for PGA and response spectra with a period of 0.6 s. The risk analysis only analyses an earthquake Mw 6.0 at 17.5 km of distance.

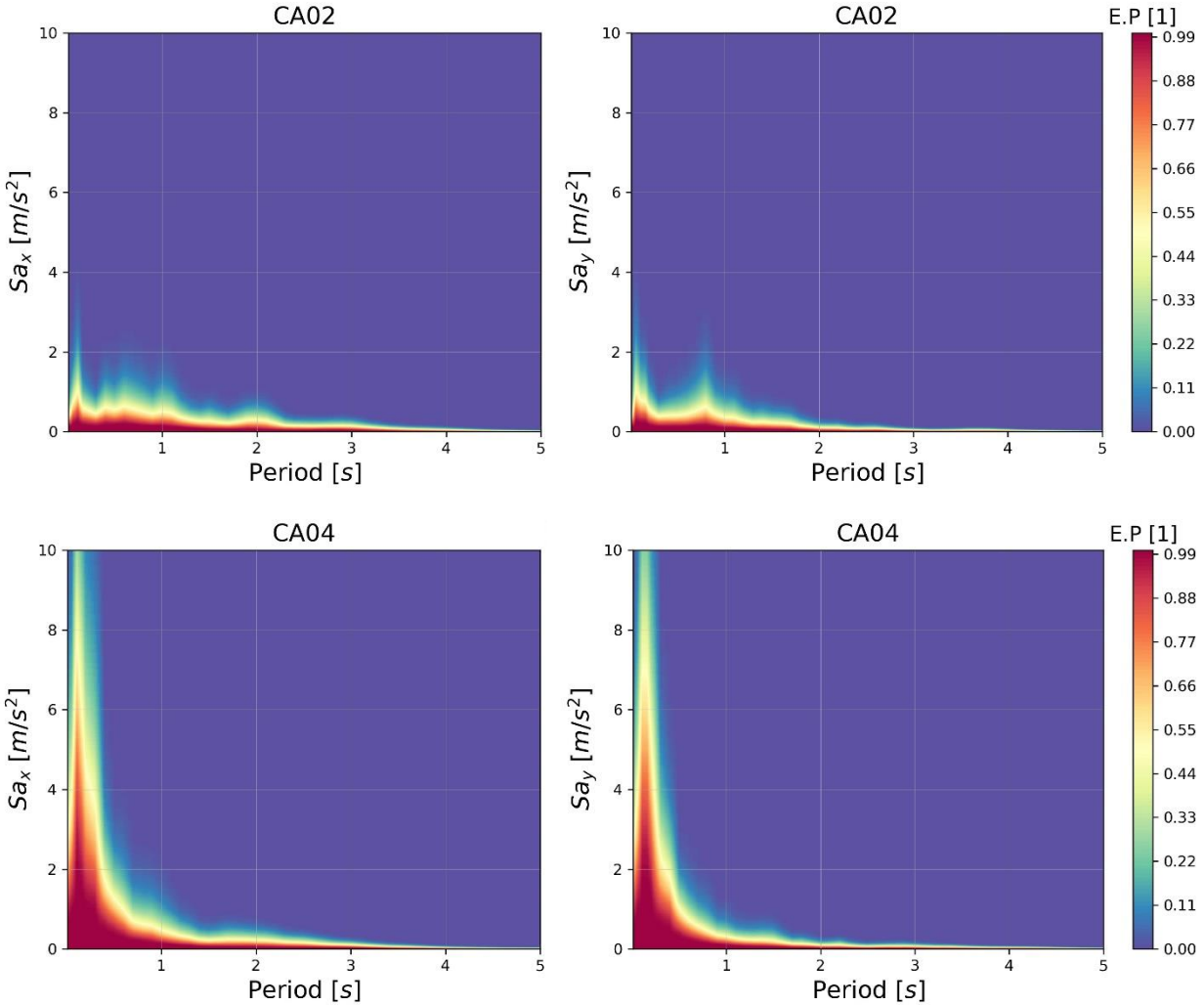

Fig. 14 - Exceedance probability (E.P) of response spectra at the stations CA04 (top) and CA02 (bottom). The average value corresponds to E.P equal 0.5. Summing and removing the standard deviation, it corresponds to E.P = 0.84 and E.P = 0.16.

5. Acknowledgements

This work, within the SINAPS@ project, benefited from French state funding managed by the National Research Agency under program RNSR Future Investment bearing reference No. ANR-11-RSNR-0022-04. The research reported in this paper has been supported in part by the SEISM Paris, Saclay Research institute.

This work was granted access to the HPC resources of CINES under the allocation 2018-A0040410444 made by GENCI. Computations were also performed using HPC resources from the computing center of Centrale Supelec supported by Centrale Supelec and CNRS.

We also acknowledge CEA for providing the geologic data of this study.

6. Conclusions

We reproduce an earthquake Mw 6.0 at 17.5 km away from the structures of Cadaracahe (see Fig. 1). We follow the method of EGF generating random Fc (including the variability of the stress drop) [9] for creating multiple possible sources. Continuously we obtain the possible ground motions at Cadarache zone using records of weak earthquakes as EGF. Those simulations have a frequency range between 2 Hz to 15 Hz because the quality of the record of the weak ground motions.

We model the same sources by Green function method but using a synthetic records, instead of weak ground motions. We computed the synthetic records using Spectral element method [4], including topographic and complex geology 3D effects in the model. Using those synthetic records (SGF), we use them as Green's function to recreate the ground motions for the same sources we did with the EGF. In this case the frequency range of the model is between 0.03 Hz to 4 Hz. Using SGF we can obtain ground motions with different sources with lower computational cost than an entire simulation using SEM with the same frequency band (see Fig. 8 and Fig. 9).

We propose a procedure to joint SGF ground motions and EGF and obtain a ground motion with a wide frequency range. Since we can model several configuration of sources with lower computational cost, than SEM method for example, we simulate 5000 ground motions taking in account the source variability. Those simulations have a wide frequency range between 0.03 Hz to 15 Hz. The analysis of those simulation allows us to compute the seismic risk at the zone of Cadarache (see Fig. 14). The zone has a 50 % of probability to have an PGA upper than 1.4 m/s^2 and 7.5 m/s^2 in the outcrop and in the basin respectively.

7. References

[1] Kohrs-Sansorny C, Courboulex F, Bour M, Deschamps A. A Two-Stage Method for Ground-Motion Simulation Using Stochastic Summation of Small Earthquakes. Bulletin of the Seismological Society of America 2005;95:1387–400. https://doi.org/10.1785/0120040211.

[2] Ripperger J, Mai PM, Ampuero J-P. Variability of Near-Field Ground Motion from Dynamic Earthquake Rupture SimulationsVariability of Near-Field Ground Motion from Dynamic Earthquake Rupture Simulations. Bulletin of the Seismological Society of America 2008;98:1207–28. https://doi.org/10.1785/0120070076.

[3] Maufroy E, Chaljub E, Hollender F, Bard P-Y, Kristek J, Moczo P, et al. 3D numerical simulation and ground motion prediction: Verification, validation and beyond–Lessons from the E2VP project. Soil Dynamics and Earthquake Engineering 2016;91:53–71.

[4] Cupillard P, Delavaud E, Burgos G, Festa G, Vilotte J-P, Capdeville Y, et al. RegSEM: a versatile code based on the spectral element method to compute seismic wave propagation at the regional scale. Geophys J Int 2012;188:1203–20. https://doi.org/10.1111/j.1365-246X.2011.05311.x.

[5] Guyonnet-Benaize C, Lamarche J, Hollender F, Viseur S, Münch P, Borgomano J. Three-dimensional structural modeling of an active fault zone based on complex outcrop and subsurface data: The Middle

Durance Fault Zone inherited from polyphase Meso-Cenozoic tectonics (southeastern France). Tectonics 2015;34:265–89. https://doi.org/10.1002/2014TC003749.

[6] Hartzell SH. Earthquake aftershocks as Green's functions. Geophysical Research Letters 1978;5:1–4.

[7] Courboulex F, Vallée M, Causse M, Chounet A. Stress-Drop Variability of Shallow Earthquakes Extracted from a Global Database of Source Time Functions. Seismological Research Letters 2016;87:912–8. https://doi.org/10.1785/0220150283.

[8] Vallée M, Charléty J, Ferreira AMG, Delouis B, Vergoz J. SCARDEC: a new technique for the rapid determination of seismic moment magnitude, focal mechanism and source time functions for large earthquakes using body-wave deconvolution. Geophys J Int 2011;184:338–58. https://doi.org/10.1111/j.1365-246X.2010.04836.x.

[9] Castro-Cruz D. Empirical prediction of seismic strong ground motion : contributions to the nonlinear soil behavior analysis and the Empirical Green's function approach. phdthesis. Université Côte d'Azur, 2018.

[10] Dujardin A, Hollender F, Causse M, Berge-Thierry C, Delouis B, Foundotos L, et al. Optimization of a Simulation Code Coupling Extended Source (k−2) and Empirical Green's Functions: Application to the Case of the Middle Durance Fault. Pure Appl Geophys 2019. https://doi.org/10.1007/s00024-019-02309-x.

[11] Festa G, Vilotte J-P. The Newmark scheme as velocity-stress time-staggering: an efficient PML implementation for spectral element simulations of elastodynamics. Geophysical Journal International 2005;161:789–812. https://doi.org/10.1111/j.1365-246X.2005.02601.x.

[12] Kristeková M, Kristek J, Moczo P, Day SM. Misfit Criteria for Quantitative Comparison of Seismograms. Bulletin of the Seismological Society of America 2006;96:1836–50. https://doi.org/10.1785/0120060012.

[13] Kristeková M, Kristek J, Moczo P. Time-frequency misfit and goodness-of-fit criteria for quantitative comparison of time signals. Geophys J Int 2009;178:813–25. https://doi.org/10.1111/j.1365-246X.2009.04177.x.

[14] Aki K. Scaling law of seismic spectrum. Journal of Geophysical Research 1967;72:1217–31.

[15] Brune J. Correction (to Brune, 1970). J Geophys Res 1971;76:5002.

